

Dynamics of the Formation of an Electron Bubble in Liquid Helium

Michael Rosenblit and Joshua Jortner

School of Chemistry, Tel-Aviv University, Ramat Aviv, Tel-Aviv 69978, Israel

(Received 7 August 1995)

The dynamics of excess electron localization in a bubble (equilibrium radius 17 \AA) in liquid He is described in terms of the initial formation of an incipient bubble of radius 3.5 \AA , followed by an adiabatic bubble expansion in the ground electronic state, which is described by a hydrodynamic model for the expansion of a spherical cavity in an incompressible liquid. The bubble expansion time at pressure $P = 0$ in liquid ^4He is $\tau_b = 3.9 \text{ ps}$; the expansion time exhibits a marked pressure dependence (e.g., $\tau_b = 1.5 \text{ ps}$ at $P = 16 \text{ atm}$) and a small (3%) isotope effect in liquid ^3He . The interrogation of the electron bubble dynamics by femtosecond absorption spectroscopy is analyzed.

PACS numbers: 67.40.Fd, 67.40.Yv, 71.70.Ms

The interaction between an electron and a helium atom is strongly short-range repulsive, with a very weak long-range attractive polarization interaction [1,2]. Accordingly, the conduction band energy for an excess quasifree electron in liquid helium is large and positive, i.e., $V_0 \cong 1.0 \text{ eV}$, above the vacuum level [3–9]. A local fluid dilation leads to a localized state of the excess electron whose total energy is located below the conduction band [10–18]. The delocalized, unstable quasifree excess electron state decays into the localized “electron bubble” state, with the electron being confined to a cavity (with a radius of $R_b \sim 17 \text{ \AA}$) in the liquid [11–18]. Extensive theoretical [11–15,17,18] and experimental [10,14,16,18] studies provided a coherent physical picture of the structure, energetics, and spectroscopy of the electron bubble in liquid helium, which involve its energetic stability [6,11,12,18], its radius [11–15,18], its compressibility [13], the “critical” density for electron localization in dense He gas [11], electron localization in solid helium [19], the energetics [15–17], and the line broadening [16,17] of the bound-bound electronic transitions and the photoionization threshold [14,15]. Of considerable interest is the dynamics of excess electron localization in liquid and fluid helium [20–25], which constitutes the subject matter of this paper. The instability of the conduction band quasifree excess electron state, which leads to the bubble formation, pertains to electron localization accompanied by large configurational changes in bulk dense helium fluid, in other dense fluids consisting of light and saturated atoms or molecules, i.e., ^3He [10–20], H_2 and D_2 [20], and Ne [5,12] and also presumably in some large finite systems, e.g., internal excess electron localization in large clusters of ^4He [20,21]. Experimental information on the time scale of the relaxation of a quasifree electron to form the electron bubble in liquid helium emerged from electron injection experiments of Hernandez and Silver [22,23], which indicated that an energetic ($\sim 1 \text{ eV}$) electron relaxes to a bubble state within a time $\tau \sim 2 \times 10^{-12} \text{ s}$. Jiang, Kim, and Northby [20] provided a rough estimate of the characteristic time for bubble

formation in terms of $\tau \sim R_b/v_s$, where $R_b = 17 \text{ \AA}$ is the bubble radius and $v_s = 240 \text{ ms}^{-1}$ is the speed of sound resulting in $\tau \sim 7 \times 10^{-12} \text{ s}$. On the other hand, the semiclassical surface hopping trajectory method calculations [25] provided a time scale of $(2-3) \times 10^{-13} \text{ s}$ for electron cavity formation in high density ($\rho^* = 0.9$) He gas at $T = 309 \text{ K}$.

We address the time-resolved dynamics of the electron bubble formation in liquid He, considering the adiabatic process where the strongly repulsive electron-helium interaction drives out a large number of atoms towards regions where the electron density is low, while the electron is localized within the fluid dilation where the helium density is negligible. We describe the electron bubble dynamics by a hydrodynamic model for the cavity expansion. This hydrodynamic model constitutes the reverse situation of the Rayleigh model [26] for a cavity collapse in a liquid induced by external pressure. The Rayleigh model for a cavity collapse was recently advanced and developed by Rips [27] for the description of the solvation dynamics of the solvated electron in water, where cavity contraction in the polar liquid is induced by long-range attractive polarization (large polaron) interactions. In our hydrodynamic model for the electron bubble dynamics the cavity expansion is induced by the electron-atom short-range repulsion, and by the decreased kinetic energy of the electron, and counteracted by the contractible force on the bubble resulting from surface tension and by the pressure-volume work involved in the creation of the bubble. The results of our calculations for the electron bubble dynamics in liquid helium will be supplemented by the calculation of the time-resolved spectra, making contact with experimental reality.

The adiabatic potential energy surfaces [15,24] for the ground ($1s$) electronic state and for the quasifree excess electron state (Fig. 1) can be obtained from the Wigner-Seitz (WS) model [5,11,13,28,29]. The electronic energy V_0 of a quasifree electron state is $V_0 = \hbar^2 k_0^2/2m + 2\pi\rho a\hbar^2/m - (8\pi^2/3)\alpha e^2\rho^{4/3}F$, where ρ is the solvent density, $a \cong -0.01 \text{ \AA}$ the single atom polar-

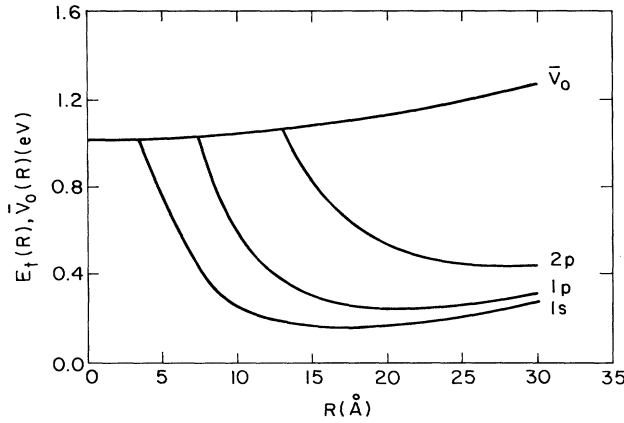


FIG. 1. Configurational diagrams for the ground electronic state $E_t^{1s}(R)$, for the bound excited electronic states $E_t^{1p}(R)$ and $E_t^{2p}(R)$, and for the quasifree electron state $\bar{V}_0(R) = V_0 + E_b(R)$ in liquid He at $P = 0$ (see text).

izability scattering length [28,29], $F = (1 + 8\pi\alpha\rho/3)^{-1}$ is the screening factor with the atomic polarizability α , and k_0 is obtained from the WS condition [5,11,13]. The total energy of a quasifree state with an empty cavity of radius R in the liquid is $\bar{V}_0(R) = V_0 + E_b(R)$. The bubble energy [5,11–18] is $E_b(R) = 4\pi R^2\gamma + (4\pi/3)PR^3 - (e^2/2R)(1 - 1/\epsilon)$, where γ is the surface tension, P is the external pressure, and ϵ is the dielectric constant. The total energy $E_t^{1s}(R) = E_e^{1s}(R) + E_b(R)$, with the electronic energy $E_e^{1s}(R)$ being obtained by the procedure of Springett, Cohen, and Jortner [13], with $E_e^{1s}(R) = (\hbar\kappa X)^2/2m$, where $\kappa = (2mV_0/\hbar^2)^{1/2}$ and X is obtained from the boundary condition $\cotan(X\kappa R) = -(1 - X)^{1/2}/X$. The crossing of the potential energy surfaces for the quasifree electron state $\bar{V}_0(R)$ and of the localized ground state $E_t^{1s}(R)$, i.e., $E_e^{1s}(R) = V_0$, is exhibited for $P = 0$ (Fig. 1) at the cavity radius $R_0 = 3.5 \text{ \AA}$, which constitutes the incipient cavity radius for electron localization. R_0 exceeds the lower limit $R_>$ of the cavity radius for the attainment of a localized state determined by the condition [5], $\pi/2 \leq X\kappa R_>$, which gives $R_> = 3.0 \text{ \AA}$ (for $P = 0$), whereupon $R_0 > R_>$. Our value of $R_0 = 3.5 \text{ \AA}$ is in reasonable agreement with the experimental estimate of Hernandez and Silver [22,23], $R_0 \sim 4 \text{ \AA}$.

We describe the dynamics of the electron bubble formation on the basis of the following assumptions: (a) The initial electron localization in the incipient bubble of radius R_0 is fast on the time scale of the equilibrium bubble formation. Initial electron localization in high density He gas at 309 K treated by surface hopping calculations [25] occurs on the time scale of 50–100 fs, providing an *a posteriori* justification for this assumption. (b) The equilibrium configuration of the bubble, which is characterized by radius R_b , is reached by its expansion, with the spherical shape being retained during the expansion process.

(c) The bubble radius R is the reaction coordinate for the adiabatic process. (d) The liquid helium is described as an incompressible continuum. (e) Energy dissipation accompanying the bubble expansion is neglected. Our assumption that the cavity retains its spherical shape during the expansion process results in the potential flow of the solvent outside the center, which is described by the Euler equation

$$\frac{\partial v(r)}{\partial t} + v \frac{\partial v(r)}{\partial r} + \frac{1}{\rho} \frac{\partial p(r)}{\partial r} = 0, \quad (1)$$

where $v(r)$, $p(r)$, and ρ are the local radial velocity, the local pressure, and the density, respectively. The cavity expansion time $\tau(R)$ from the initial cavity radius R_0 to R ($\leq R_b$) is given by the first passage time

$$\tau(R) = \int_{R_0}^R dR' / V(R'), \quad (2)$$

where $V(R')$ is the velocity of the cavity boundary. The incompressibility of the liquid implies the continuity condition $r^2 v(r) = R^2 V(R)$, so that the kinetic energy K of the liquid is

$$K(R) = (\rho/2) \int_R^\infty dr 4\pi r^2 [v(r)]^2 = 2\pi\rho [V(R)]^2 R^3. \quad (3)$$

In the absence of energy dissipation, energy conservation implies that the kinetic energy of the liquid equals the total change of the free energy, $\Delta F(R)$, of the bubble expansion process

$$K(R) = \Delta F(R) = \bar{V}_0(R_0) - E_t^{1s}(R). \quad (4)$$

Equations (2)–(4) result in

$$\tau(R) = (2\pi\rho)^{1/2} \int_{R_0}^R dR' R'^{3/2} [\bar{V}_0(R_0) - E_t^{1s}(R')]^{-1/2}. \quad (5)$$

The expansion time for the attainment of the equilibrium bubble radius (i.e., $R = R_b$ is $\tau_b = \tau(R_b)$).

For liquid ^4He (denoted by He) at $P = 0$, we take $\gamma = 0.36 \text{ erg cm}^{-2}$ [30], $\rho = 0.0218 \text{ \AA}^{-3}$, $\epsilon = 1.0588$ [31], and obtain $V_0 = 1.02 \text{ eV}$ (experimental value $V_0 = 1.05 \pm 0.05 \text{ eV}$ [18,32]), $R_b = 17 \text{ \AA}$, and $R_0 = 3.5 \text{ \AA}$. Equation (5) results in $\tau_b = 3.89 \text{ ps}$. τ_b calculated herein from the hydrodynamic model in liquid He ($T = 4 \text{ K}$) is longer by a numerical factor of 20–40 than the surface hopping computation estimate [25] of 100–200 fs for the electron cavity formation time in high density ($\rho^* = 0.9$) high temperature He gas ($T = 309 \text{ K}$). Our theoretical result $\tau_b = 3.9 \text{ ps}$ in liquid He is in accord with the experimental estimate [22,23] of $\tau_b \sim 2 \text{ ps}$. To assess the isotope effect on the localization dynamics we calculate τ_b for liquid ^3He at $P = 0$ with the parameters $\gamma = 0.17 \text{ erg cm}^{-2}$, $\rho = 0.0162 \text{ \AA}^{-3}$, $\epsilon = 1.0428$ [5,13,29] resulting in $V_0 = 0.90 \text{ eV}$ (experimental value $1.0 \pm 0.2 \text{ eV}$

[31]), $R_b = 19.0 \text{ \AA}$, and $R_0 = 3.7 \text{ \AA}$, and yielding $\tau_b = 3.97 \text{ ps}$. The small (3%) increase of τ_b in ${}^3\text{He}$ relative to ${}^4\text{He}$ reflects the cancellation between the $\rho^{1/2}$ density effects [27], which, according to Eq. (5) decreases $\tau(R)$ by $[\rho({}^3\text{He})/\rho({}^4\text{He})]^{1/2} \cong 0.86$ and the larger R_b in liquid ${}^3\text{He}$, which increases τ_b . Of considerable interest are the effects of the electron bubble compressibility (with R_b shrinking from $R_b = 17 \text{ \AA}$ for $P = 0$ to $R_b = 12 \text{ \AA}$ for $P = 16 \text{ atm}$ [13,24]) on its formation dynamics. Utilizing the Amit-Gross formula for γ [33], we find that τ_b decreases from 3.89 ps at $P = 0$ to 1.47 ps at $P = 16 \text{ atm}$, the major effect of shortening of τ_b being due to the decrease of R_b at higher pressures (Fig. 2).

The dynamics of the expansion of the electron bubble radius from R_0 to R_b (Fig. 3) is nearly exponential. The time τ_b for the electron bubble expansion is considerably shorter than the collapse time τ_c for the collapse of the empty bubble (of the initial radius R_b), which can be formed by the adiabatic photoionization of the electron bubble. τ_c is given by Eq. (5) with $V_0 = 0$ and $E_t^{1s}(R) = 0$ for all R whereupon

$$\tau_c = (2\pi\rho)^{1/2} \int_{R_b}^0 dR' R'^{3/2} / [E_b(R_b) - E_b(R')]^{1/2}. \quad (6)$$

From the (nonexponential) time evolution of the collapse of the empty bubble (Fig. 3) we assert that $\tau_c = 19.5 \text{ ps}$. Accordingly, the decrease of the electron kinetic energy favors the electron bubble expansion considerably, speeding it up relatively to the contraction of the empty bubble.

To provide predictions for the experimental observation of this new class of dynamic processes, we explored the time-resolved spectra of the electron bubble. The potential energy surfaces $E_t^{1s}(R)$ and \bar{V}_0 were supplemented (Fig. 1) by the potential surfaces of the bound excited $1p$ and $2p$ electronic states, which were calculated by a numerical integration of the equation of Springett, Jort-

ner, and Cohen [5,13] for a particle in a spherical well. Following the adiabatic expansion of the electron bubble in the ground electronic state the allowed $1s \rightarrow 1p$ and $1s \rightarrow 2p$ electronic transitions will be exhibited. The time evolution of the absorption band maxima for these spectra (Fig. 4) exhibits an incubation time that is 0.5 ps for the $1s \rightarrow 1p$ transition and 1.65 ps for the $1s \rightarrow 2p$ transition, followed by the onset of the electronic spectra, with the peak energy $\Delta E(1s \rightarrow j)$; $j = 1p, 2p$ decreasing with time for both the $1s \rightarrow 1p$ and $1s \rightarrow 2p$ transitions, and converging to the equilibrium ($R = R_b$) excitation energies [15–17], which we calculate as $\Delta E(1s \rightarrow 1p) = 0.106 \text{ eV}$ and $\Delta E(1s \rightarrow 2p) = 0.512 \text{ eV}$ at $\tau_b \cong 3.9 \text{ ps}$ (Fig. 4). These electronic excitations, which are expected to be characterized by high oscillator strengths ($f \cong 0.1\text{--}0.9$) [34], will provide the experimental arsenal for the study of the temporal dynamics of electron localization induced and accompanied by large configurational changes, which can be interrogated by ultrafast femtosecond laser spectroscopy [35].

Our analysis of the electron bubble dynamics should be extended to account for energy dissipation in the cavity expansion, which is associated with viscosity effects and emission of sound waves, and which drives the system towards equilibrium. Accordingly, our calculations provide a lower limit for τ_b . The lengthening (by a numerical factor of ~ 2 [34]) of τ_b due to the dissipation will decrease the fluid expansion velocity (for $R = 7\text{--}10 \text{ \AA}$) below the value of v_s , rendering the incompressible continuum description of the fluid adequate.

The adiabatic electron bubble expansion can be envisioned as a dynamic solvation process of an excess electron in liquid He. In contrast to the solvation dynamics of an excess electron [36–38] or of a giant dipole [39] in polar solvents, which is dominated by short-range short-

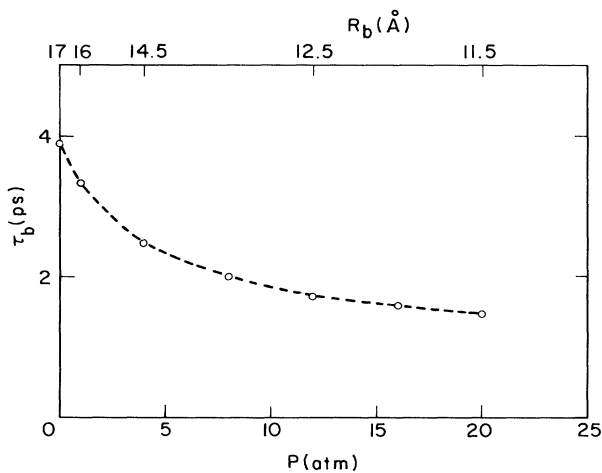


FIG. 2. The pressure dependence ($p = 0\text{--}20 \text{ atm}$) of the bubble expansion time τ_b . The equilibrium radii R_b of the electron bubble are also marked.

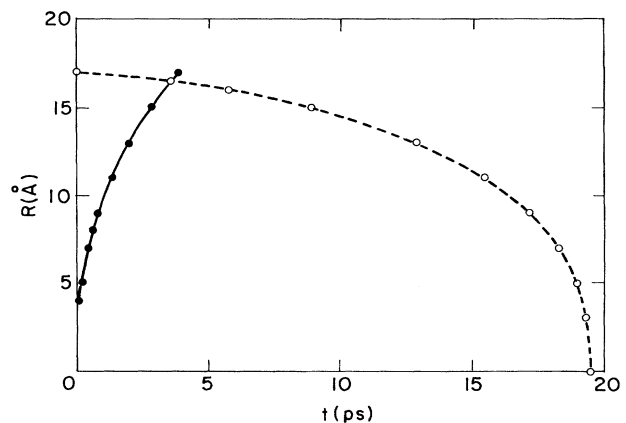


FIG. 3. Bubble dynamics in liquid He at $P = 0$. The time dependence of the increase of the radius R for the expansion of the electron bubble from $R_0 = 3.5 \text{ \AA}$ at $t = 0$ to $R_b = 17 \text{ \AA}$ at $\tau_b = 3.9 \text{ ps}$ (solid points), and the time dependence of the decrease of the radius R for the collapse of the empty bubble from R_b at $t = 0$ to $R = 0$ (open points).

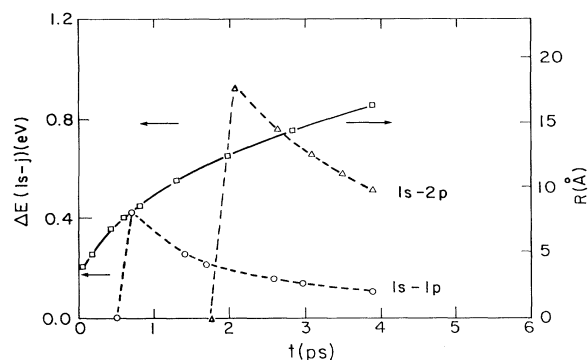


FIG. 4. The time evolution of the vertical electronic transition energies for the bound-bound $1s \rightarrow 1p$ (open dots) and $1s \rightarrow 2p$ transitions (open triangles). The time dependence of the electron bubble radius (squares connected by a solid curve) R is also shown.

time angular relaxation of the solvent molecules driven by inertial motion [36–40], the electron bubble formation in liquid He involves a short-time radial expansion process.

We are indebted to Dr. Ilya Rips for stimulating discussions and for communicating to us the results of his work (Ref. [27]) prior to publication. This research was supported by the Deutsche Forschungsgemeinschaft (Sonderforschungsbereich 377).

- [1] N. Kestner, J. Jortner, M. H. Cohen, and S. A. Rice, *Phys. Rev.* **140**, A56 (1965).
- [2] M. V. Rama Krishna and K. B. Whaley, *Phys. Rev. B* **38**, 11 839 (1988).
- [3] W. T. Sommer, *Phys. Rev. Lett.* **12**, 271 (1964).
- [4] M. A. Woolf and G. W. Rayfield, *Phys. Rev. Lett.* **15**, 235 (1965).
- [5] B. R. Springett, J. Jortner, and M. H. Cohen, *J. Chem. Phys.* **48**, 2720 (1968).
- [6] J. R. Broomall, W. D. Johnson, and D. G. Onn, *Phys. Rev. B* **14**, 2919 (1976).
- [7] B. Plenkiewicz, P. Plenkiewicz, and J. P. Jay-Gerin, *Chem. Phys. Lett.* **163**, 542 (1989).
- [8] K. Martini, J. P. Toennies, and C. Winkler, *Chem. Phys. Lett.* **178**, 429 (1991).
- [9] B. Space, D. Coker, Z. Liu, B. J. Berne, and G. Martyna, *J. Chem. Phys.* **97**, 2002 (1992).
- [10] L. Meyer and F. Reif, *Phys. Rev.* **119**, 1164 (1960).
- [11] J. Jortner, N. R. Kestner, M. H. Cohen, and S. A. Rice, *J. Chem. Phys.* **43**, 2614 (1965); K. Hiroike, N. R. Kestner, S. A. Rice, and J. Jortner, *J. Chem. Phys.* **43**, 2625 (1965).
- [12] W. B. Fowler and D. L. Dexter, *Phys. Rev.* **176**, 337 (1976).
- [13] B. E. Springett, M. H. Cohen, and J. Jortner, *Phys. Rev.* **159**, 183 (1967).
- [14] J. A. Northby and T. M. Sanders, *Phys. Rev. Lett.* **18**, 1184 (1967).
- [15] T. Miyakawa and D. L. Dexter, *Phys. Rev. A* **1**, 513 (1970).
- [16] C. C. Grimes and G. Adams, *Phys. Rev. B* **41**, 6366 (1990); **45**, 2305 (1992).
- [17] A. Ya. Parshin and V. Pereverzev, *Sov. Phys. JETP* **74**, 68 (1992).
- [18] A. L. Fetter, in *The Physics of Liquid and Solid Helium*, edited by K. H. Benneman and J. B. Ketterson (Wiley, New York, 1976), pp. 1 and 207.
- [19] M. H. Cohen and J. Jortner, *Phys. Rev.* **180**, 238 (1969).
- [20] T. Jiang, C. Kim, and J. A. Northby, *Phys. Rev. Lett.* **71**, 700 (1993).
- [21] J. A. Northby, C. Kim, and T. Jian, *Physica (Amsterdam)* **197B**, 426 (1994).
- [22] J. P. Hernandez and M. Silver, *Phys. Rev. A* **2**, 1949 (1970).
- [23] J. P. Hernandez and M. Silver, *Phys. Rev. A* **3**, 2152 (1971).
- [24] J. Jortner, *Ber. Bunsen-Ges. Phys. Chem.* **75**, 696 (1971).
- [25] B. Space and D. F. Coker, *J. Chem. Phys.* **94**, 1976 (1991); **96**, 652 (1992).
- [26] J. W. Strat (Lord Rayleigh), *Philos. Mag.* **34**, 94 (1917).
- [27] I. Rips, "Electron Solvation Dynamics in Polar Solvents" (to be published).
- [28] E. Cheng, M. W. Cole, and M. H. Cohen, *Phys. Rev. B* **50**, 1136 (1994); **50**, 16 134 (1994).
- [29] M. Rosenblit and J. Jortner, *J. Chem. Phys.* **101**, 8039 (1994); *Phys. Rev. B* (to be published).
- [30] V. R. Pandharipande, S. C. Pieper, and R. B. Wiringa, *Phys. Rev. B* **34**, 4571 (1986).
- [31] M. W. Cole, *Phys. Rev. B* **2**, 4239 (1970); **3**, 4418 (1971).
- [32] K. Martini, J. P. Toennies, and C. Winkler, *Chem. Phys. Lett.* **178**, 429 (1991).
- [33] D. Amit and E. P. Gross, *Phys. Rev.* **145**, 130 (1966).
- [34] M. Rosenblit and J. Jortner (to be published).
- [35] *Ultrafast Phenomena VIII*, edited by J. L. Martin, A. Migus, G. A. Mourou, and A. H. Zewail (Springer-Verlag, Berlin, 1993).
- [36] E. Neria, A. Nitzan, R. N. Barnett, and U. Landman, *Phys. Rev. Lett.* **67**, 1011 (1991).
- [37] A. Migus, J. Martin, and A. Antonetti, *Phys. Rev. Lett.* **58**, 1559 (1987).
- [38] J. Alfano, P. Wallhout, Y. Kimura, and P. Barbara, *J. Chem. Phys.* **98**, 5996 (1993).
- [39] S. J. Rosenthal, X. Xie, M. Du, and G. R. Fleming, *J. Chem. Phys.* **95**, 4715 (1991).
- [40] I. Rips and J. Jortner, *J. Chem. Phys.* **87**, 2090 (1987).